Received: 4 December 2020 | Revised: 19 January 2021 | Accepted: 22 January 2021

DOI: 10.1111/mmi.14687

RESEARCH ARTICLE

WILEY

Conserved lysine residues in decorin binding proteins of *Borrelia garinii* are critical in adhesion to human brain microvascular endothelial cells

Annukka Pietikäinen[1,2] | Mia Åstrand[3,4] | Julia Cuellar[1] | Otto Glader[1,5] | Heli Elovaara[1] | Meri Rouhiainen[1,5] | Jemiina Salo[1] | Tomomi Furihata[6] | Tiina A. Salminen[3] | Jukka Hytönen[1,2]

[1]Institute of Biomedicine, Faculty of Medicine, University of Turku, Turku, Finland

[2]Laboratory Division, Clinical Microbiology, Turku University Hospital, Turku, Finland

[3]Structural Bioinformatics Laboratory, Biochemistry, Faculty of Science and Engineering, Åbo Akademi University, Turku, Finland

[4]National Doctoral Programme in Informational and Structural Biology, Faculty of Science and Engineering, Åbo Akademi University, Turku, Finland

[5]Doctoral Programme in Clinical Research, Turku, Finland

[6]Laboratory of Clinical Pharmacy and Experimental Therapeutics, School of Pharmacy, Tokyo University of Pharmacy and Life Sciences, Tokyo, Japan

Correspondence
Annukka Pietikäinen, University of Turku, Institute of Biomedicine, Kiinamyllynkatu 10, FI-20520 Turku, Finland.
Email: kaisa.pietikainen@utu.fi

Funding information
This study was financially supported by the Academy of Finland (grant number 265098) (JH), Jane and Aatos Erkko Foundation (JH), Magnus Ehrnrooth Foundation (MÅ), the Sigrid Juselius Foundation (TAS), and the Tor, Joe, and Pentti Borg's Foundation (TAS)

Abstract

Lyme borreliosis is a tick-borne disease caused by *Borrelia burgdorferi* sensu lato spirochetes (Lyme borreliae). When the disease affects the central nervous system, it is referred to as neuroborreliosis. In Europe, neuroborreliosis is most often caused by *Borrelia garinii*. Although it is known that in the host Lyme borreliae spread from the tick bite site to distant tissues via the blood vasculature, the adherence of Lyme borreliae to human brain microvascular endothelial cells has not been studied before. Decorin binding proteins are adhesins expressed on Lyme borreliae. They mediate the adhesion of Lyme borreliae to decorin and biglycan, and the lysine residues located in the binding site of decorin binding proteins are important to the binding activity. In this study, we show that lysine residues located in the canonical binding site can also be found in decorin binding proteins of *Borrelia garinii*, and that these lysines contribute to biglycan and decorin binding. Most importantly, we show that the lysine residues are crucial for the binding of Lyme borreliae to decorin and biglycan expressing human brain microvascular endothelial cells, which in turn suggests that they are involved in the pathogenesis of neuroborreliosis.

KEYWORDS

biglycan, *Borrelia*, *Borrelia garinii*, decorin, endothelial cells, lysine

1 | INTRODUCTION

The number of reported cases of Lyme borreliosis (LB) have increased in recent years (Sajanti et al., 2017; Steere et al., 2016). The causative agents, a group of *Borrelia burgdorferi* sensu lato spirochetes (Lyme borreliae), is spread through the bites of infected ticks. If the tick is not promptly removed from the skin, Lyme borreliae can spread from the tick to the skin and cause a disease. The local sign of infection in the skin is an erythema migrans skin rash. Lyme borreliae can further spread from the skin to distant tissues and cause a multisystem

disease affecting several organs. The three most common genospecies causing LB are *B. burgdorferi* sensu stricto (Bbss), *B. garinii* (Bg), and *B. afzelii* (Ba). Bbss causes most of the LB cases in North America while in Europe Bg and Ba are the dominant genospecies. Bbss is mainly associated with arthritis, Ba with the skin disorder acrodermatitis chronica atrophicans and Bg is associated with neuroborreliosis (Steere et al., 2016).

Lyme borreliae spread in the host via the blood vasculature (Moriarty et al., 2008) and are able to bind vascular endothelial cells (Coburn et al., 1998, 2013; Salo et al., 2016). Once Lyme borreliae make the initial adherence contact with the endothelium they are able to transmigrate across the endothelium and reach the distant tissues (Moriarty et al., 2008; Norman et al., 2008). There are a few studies where it has been shown that Lyme borreliae are also able to transmigrate across the endothelial barrier of the brain microvasculature (Bista et al., 2020; Grab et al., 2005, 2009; Nyarko et al., 2006; Pulzova et al., 2011), while no studies have been published on the initial adhesion of Lyme borreliae to human brain microvascular endothelial cells (HBMECs).

Vascular interactions and adherence are mediated through multiple adhesins located on the outer surface of Lyme borreliae (Brissette & Gaultney, 2014). Decorin binding proteins A and B (DbpA, DbpB; Dbps) are surface-localized adhesins of Lyme borreliae expressed during mammalian infection (Brissette & Gaultney, 2014; Lin et al., 2017). The Dbps mediate binding to the proteoglycans decorin and biglycan. Proteoglycans are glycosylated proteins with a wide range of functions in the extracellular matrix, and they bind to other proteins through electrostatic interactions mediated by the negatively charged glycosaminoglycan (GAG) chains on their surface (Gandhi & Mancera, 2008). Decorin is expressed, for example, in extracellular matrix, while biglycan, on the contrary, is expressed also on blood endothelial cells (Salo et al., 2016). Previously, we have shown that Dbps of Bg bind biglycan on endothelial cells under flow conditions that mimic the blood flow in the vasculature (Salo et al., 2016).

The amino acid sequences of DbpA are more heterogeneous between different Lyme borreliae genospecies and strains compared to sequences of DbpB, which are conserved (Heikkilä et al., 2002a, 2002b; Roberts et al., 1998). However, the tertiary structures of mature Dbps are similar, consisting of five helices, a linker between helices 1 and 2, and a C-terminal tail which can vary in length (Feng & Wang, 2015). According to the published structures of Dbps of Bbss and DbpA of Bg, the Dbps share a common ligand binding site (Feng & Wang, 2015; Morgan & Wang, 2015; Wang, 2012), which is a basic patch formed by residues of helices 2 and 5 (lysines 82, 163, and 170) (Brown et al., 1999; Pikas et al., 2003). The site is referred to as the canonical GAG-binding site, and it has, in fact, been shown to be critical for decorin binding and infection of mice (Brown et al., 1999; Feng & Wang, 2015; Fortune et al., 2014; Morgan et al., 2015; Morgan & Wang, 2015; Pikas et al., 2003; Wang, 2012).

Our objective was to study whether the conserved lysine residues in DbpA and DbpB are present in Bg strains, to model the structures of the proteins and to evaluate whether the lysines in the Dbps of Bg are critical for binding to decorin and biglycan. Moreover, since Bg is known to be the main causative agent of neuroborreliosis in Europe, we wanted to analyze whether the Dbps (and the lysine residues) of Bg are important also in mediating adhesion of Lyme borreliae to human brain microvascular endothelial cells.

2 | RESULTS

2.1 | Sequence alignment and construction of mutated recombinant proteins

To assess whether the Dbps of Bg SBK40 also have lysine residues in the same positions as the previously analyzed DbpA of Bbss 297 (Brown et al., 1999), the amino acid sequences of these proteins were aligned. The alignment demonstrated that lysine 82, shown to be important for decorin binding in DbpA of Bbss 297, aligns with lysine 80 in DbpA and with lysine 79 in DbpB of Bg SBK40 (Figure 1). In addition, there are two other lysine residues, K78 and K82, close to K80 in DbpA of Bg SBK40 that are missing in DbpA of Bbss 297.

To see whether K78/80/82 in DbpA of Bg SBK40 and K79 in DbpB of Bg SBK40 are conserved among all Bg strains, we performed an alignment of published Dbp amino acid sequences of Bg strains (Supplementary Figure S1). The alignment revealed that K80 is conserved among all published sequences, whereas K78 and K82 are conserved in the majority of sequences. In the nonconserved sequences, K78 is mostly substituted for aspartate or glutamate and K82 for arginine or glutamine. In the DbpB sequences, K78 is substituted for aspartate and K82 for glutamine.

To analyze the role of these lysine residues in proteoglycan binding, we mutated K78/80/82 in DbpA of Bg SBK40 and K79 in DbpB of Bg SBK40 to alanine. Sequencing of the constructs showed that the site-directed mutagenesis was successful, and no other mutations had been formed. Wild-type (wt) and mutated recombinant Dbps were then expressed in *Escherichia coli* and purified for further analyses.

2.2 | Thermofluor analysis

Thermofluor assay was performed to evaluate whether the mutations affected the stability of the recombinant proteins. The analysis revealed that wt DbpA had a melting temperature (Tm) of 72.2°C, which was ca. 7 degrees higher than the melting temperature of mutated recombinant DbpA (Tm 65.3°C) (Supplementary Figure S2). The wt recombinant DbpB and mutated DbpB, on the contrary, had similar melting temperatures (Tm 57.6°C and 56.3°C, respectively).

2.3 | Structural analysis

To study the structural impact of the mutations and to analyze the potential binding sites, homology models were created for the Bg SBK40

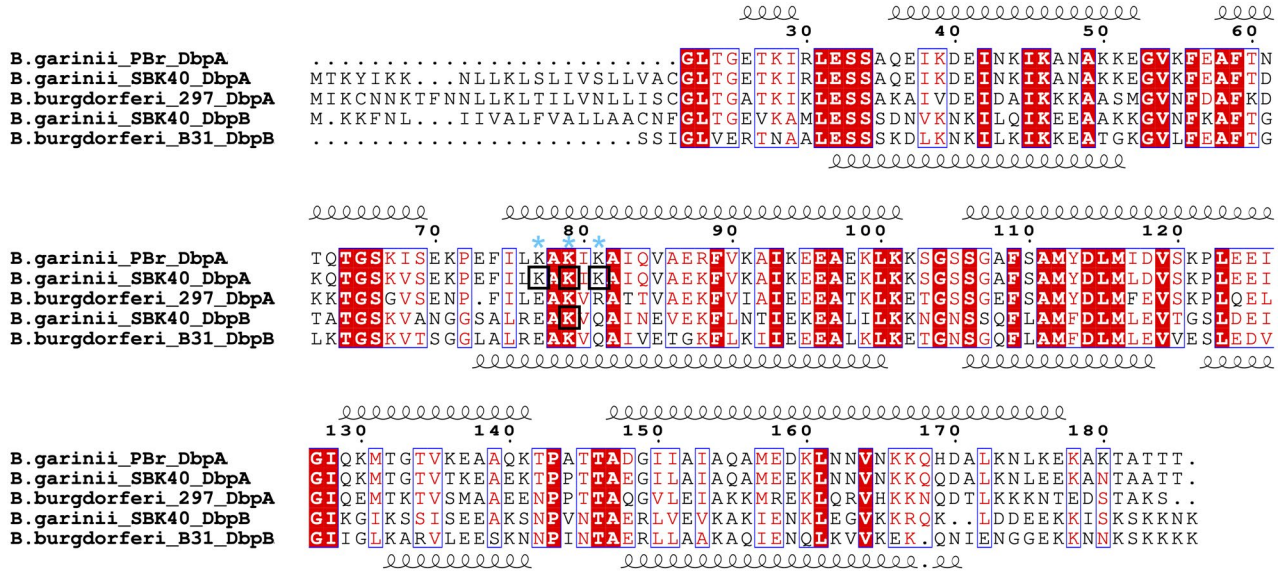

FIGURE 1 Multiple sequence alignment used for homology modeling. The Bg SBK40 DbpA and DbpB proteins are aligned to the structural templates used for modeling, Bg PBr DbpA (PDB ID: 2mtd, Morgan & Wang, 2015)) and Bbss B31 DbpB (PDB ID: 2mvg, (Feng & Wang, 2015)). The extensively studied DbpA protein of Bbss 297 is also included. The secondary structures of the templates are shown above (2mtd) and below (2mvg) the alignment. Conserved residues are shown with red background and similar residues are shown in red and boxed. The mutated residues are shown in black boxes and their positions are indicated by blue asterisks

wt DbpA and DbpB proteins and for the mutants (DbpA K78A/K80A/K82A, DbpB K79A). Homology modeling is a commonly used protein structure prediction method where the structure of an unknown protein is modeled based on the structure of a related protein (França, 2015). DbpA of Bg SBK40 shares 89.6% sequence identity with DbpA of Bg PBr ((PDB ID: 2mtd, (Morgan & Wang, 2015)) while DbpB shares 61% sequence identity with DbpB of Bbss B31 (PDB ID: 2mvg, (Feng & Wang, 2015)) and these structures were, respectively, used as structural templates for modeling the Bg SBK40 DbpA and DbpB. The models were carefully evaluated through visual inspection and by quality evaluation servers. The RMSD (root mean square deviation) to the template structures were 0.49 Å and 0.51 Å for DbpA and DbpB, respectively. The ModFOLD global model quality score was above 0.5 for both DbpA and DbpB (score > 0.4 indicates complete and confident models) and the ProQ LG scores were 4.988 and 4.724 for DbpA and DbpB, respectively (values > 4 indicates extremely good models).

Bg SBK40 DbpA and DbpB have high amino acid sequence similarity with other Dbps, and thus, share the same overall fold as previously published Dbp structures (Feng & Wang, 2015; Fortune et al., 2014; Morgan & Wang, 2015; Wang, 2012), consisting of five alpha helices and a linker region between helices 1 and 2 (Figure 2). The linker in DbpA has a helical structure, whereas in DbpB, and in most other DbpA structures, the linker forms an unstructured loop (Figure 2). In the DbpB structure, helix 5 is significantly shorter than in DbpA and the C-terminal end is, therefore, longer and more unstructured. DbpA K80 and DbpB K79 are located in the canonical binding site, whereas DbpA K78 and K82 are located on the opposite side of the protein (Figure 2). K80, K161, and K168 in DbpA and K79, K160, and R167 in DbpB correspond to the canonical GAG-binding residues.

GAGs are known to interact with Dbps through electrostatic interactions and the electrostatic surface potential of the proteins can, therefore, give a good indication of possible GAG-binding sites. The electrostatic surface potential maps of the Bg SBK40 Dbp wt and mutant proteins show that the mutations cause significant changes in the surface potentials of the Dbp proteins, which, in turn, may lead to changes in the ability to bind GAGs (Figure 3).

Since the DbpA mutant had a lower melting temperature than the wt, we performed molecular dynamics (MD) simulations to study whether the mutations affect the stability of the proteins. The 3D fold of both the wt DbpA and the DbpA mutant proteins, as well as the wt DbpB and DbpB mutant, remained intact throughout the simulations and only the terminal-regions and the linker showed more flexibility (Supplementary Figure S3). Interestingly, the linker in wt DbpB was more flexible than in the mutant DbpB (Supplementary Figure S3c), whereas no such difference could be observed for DbpA.

2.4 | Binding of recombinant proteins to biglycan and decorin

The binding of recombinant wt and mutated DbpB to biglycan and decorin in stationary conditions was studied with Western blot analysis and using a microtiter plate assay. Both analyses showed that wt DbpB bound well to both of the proteoglycans while the mutated DbpB did not show detectable binding in Western blot (Figure 4a), and in a microtiter plate assay the mutated DbpB bound both biglycan and decorin significantly less than the wt protein ($p < .05$ for biglycan, $p < .01$ for decorin) (Figure 4b).

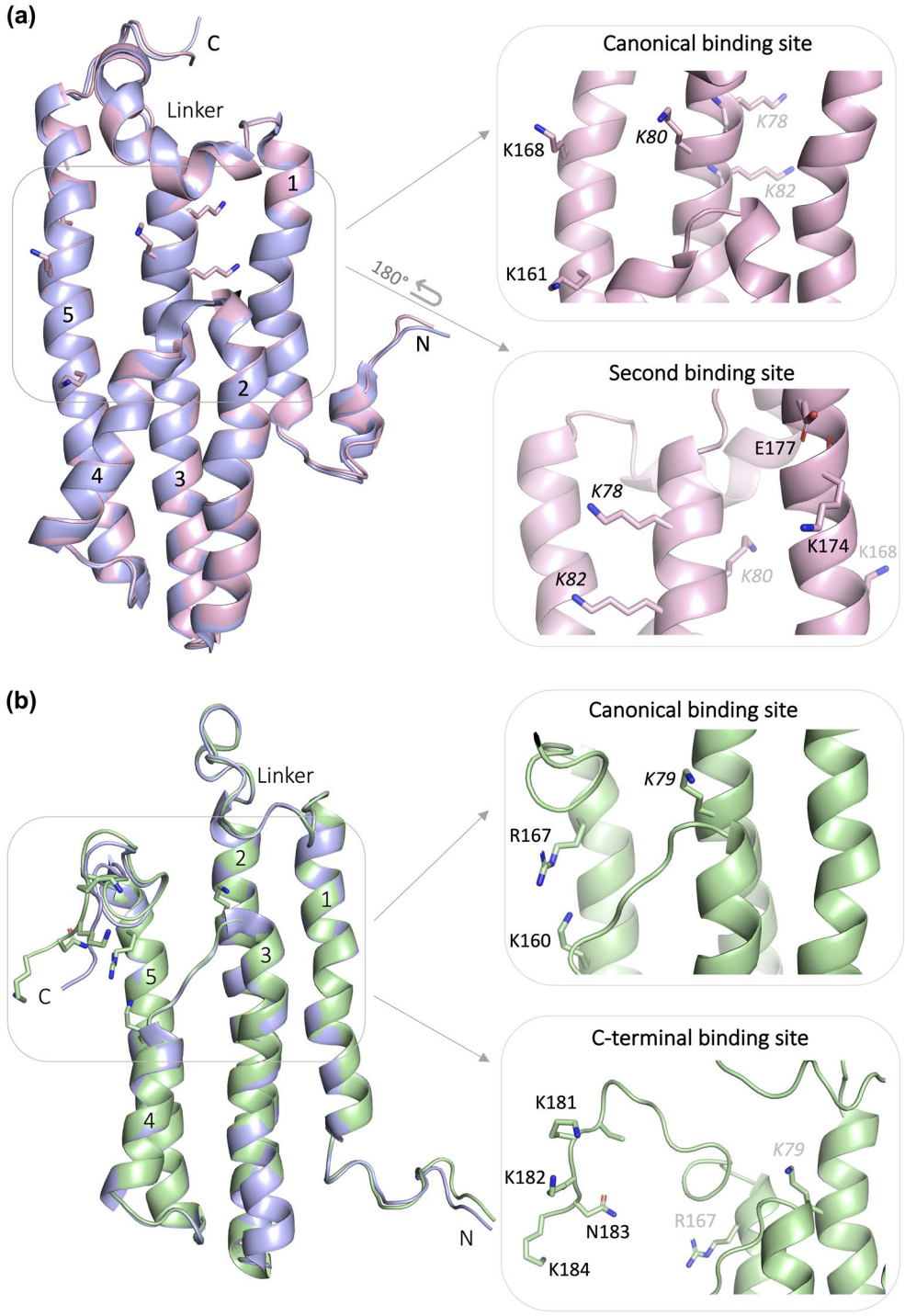

FIGURE 2 The GAG-binding sites in the 3D structures of Bg SBK40 DbpA and DbpB. (a) Bg SBK40 DbpA (pink) superimposed on the structural template (light blue) Bg PBr DbpA (PDB ID: 2mtd, (Morgan & Wang, 2015)). The close-ups show the canonical binding site, consisting of residues K80, K161, and K168, and the second binding site located on the opposite side of the protein. The second binding site shows residues K78 and K82 and residues K174 and E177, which correspond to K173 and K176 in Bg PBr DbpA (see text for more details). (b) Bg SBK40 DbpB (green) superimposed on the structural template (light blue) Bbss B31 DbpB (PDB ID: 2mvg, (Feng & Wang, 2015)). The close ups show the canonical binding site, which consist of K79, K160, and R167, and the potential second binding site located at the C-terminal end (residues K181, K182, N183, and K184). The linker of DbpB lacks the helical structure seen in DbpA and its helix 5 is shorter than in DbpA, and the C-terminal end of DbpB thus forms a longer flexible loop. The labels of the mutated residues are in italics and those located on the opposite site of the protein are in grey

The binding of DbpA to proteoglycans under stationary conditions was not studied since we have previously shown that wt DbpA of Bg SBK40 binds these proteoglycans only under flow (Salo et al., 2016). Therefore, the binding of wt and mutated Dbps to biglycan and decorin was studied under flow conditions with Biacore. In this analysis, wt DbpA bound efficiently both biglycan and decorin

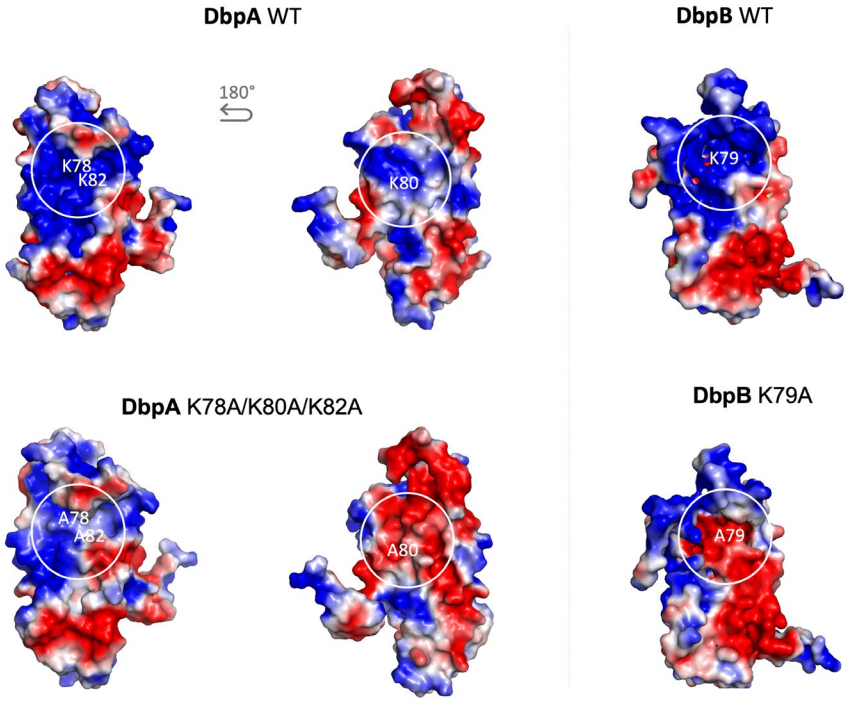

FIGURE 3 Electrostatic surface potential maps of the Bg SBK40 DbpA and DbpB models. The electrostatic surfaces were calculated with the APBS tool (Adaptive Poisson–Boltzmann Solver) in PyMOL and the color ranges from −2 (red) to 2 (blue). The lysines located on the surface of the Dbps create positively charged areas that are involved in ionic interactions with GAGs. Mutating the DbpA residues K78/K80/K82 and DbpB K79 to alanines significantly changes the surface potential of the protein and prevents GAG-binding

(Figure 4c,d). Wt DbpB also clearly bound both of these proteoglycans, although the binding was not as strong as with wt DbpA. In contrast, the mutated recombinant Dbps could not bind biglycan or decorin under flow conditions. Moreover, none of the studied Dbps bound bovine serum albumin (BSA), which served as a negative control ligand (data not shown).

2.5 | Characterization of Lyme borreliae strains expressing wt or mutated adhesins

To analyze whether the specific lysines of Dbps are critical also for the binding properties of Lyme borreliae cells, we constructed Lyme borreliae strains that either express wt Dbps of Bg SBK40 (JF105 + pME22/WTdbps), mutated Dbps (JF105 + pME22/MUTdbps), or no Dbps (JF105 + pME22) using Bbss JF105 as a background strain. Plasmid contents of the constructed strains were checked to verify that the strains had not lost any plasmids in electroporation. All of the studied strains had identical plasmid composition (Supplementary Table S1). In addition, they all contained the plasmid pME22 used in transformation.

Moreover, to verify that the wt and mutated Dbps were expressed and surface-localized, we performed Western blot analysis of proteinase K-treated bacteria. The analysis revealed that Dbps were expressed on the cells that were not treated with proteinase K because with immune serum treatment, bands with apparent molecular weight of ca. 20 kDa, corresponding the Dbps, could be visualized (Figure 5a; Proteinase K 0 μg/ml; calculated molecular weights of Dbps are 20.36 kDa for wt DbpA, 20.19 kDa for mutated DbpA, 20.06 kDa for wt DbpB, and 20.01 kDa for mutated DbpB). Proteinase K treatment diminished, although not totally abolished, the signal observed in Western blots indicating that the proteins were also surface-localized. Detection of flagella protein p41 (periplasmic location) was used as a control. Proteinase K treatment had no effect on the signal obtained with p41 antibody and, as expected, the bands were observed around 41–42 kDa in both of the experimental conditions.

2.6 | The role of conserved lysine residues in binding to biglycan, decorin, and human brain microvascular endothelial cells

The binding of the constructed JF105 strains to biotinylated biglycan and decorin was analyzed with a dot blot assay. The results showed that only the strain expressing wt Dbps was able to bind the proteoglycans, while the strain expressing the mutated Dbps and the strain containing the pME22 expression plasmid only did not show any decorin or biglycan binding (Figure 5b).

Finally, to evaluate whether the Dbps (and the lysines) are critical for binding of Lyme borreliae to human endothelial cells, we performed adhesion studies with the constructed JF105 strains and HBMECs. First, we analyzed biglycan and decorin expression on HBMECs with flow cytometry. The analysis revealed that the cells, indeed, expressed both of these proteoglycans. Representative figures of the experiments are shown in Figure 6a,b. Mean fluorescence intensities of samples treated with biglycan or decorin antibodies were compared to samples treated with isotype control antibody or to samples where only secondary antibody had been used for staining. Mean fluorescence intensities were statistically significantly stronger in samples treated with decorin or biglycan antibodies compared to the controls (Figure 6c). Next, transformed

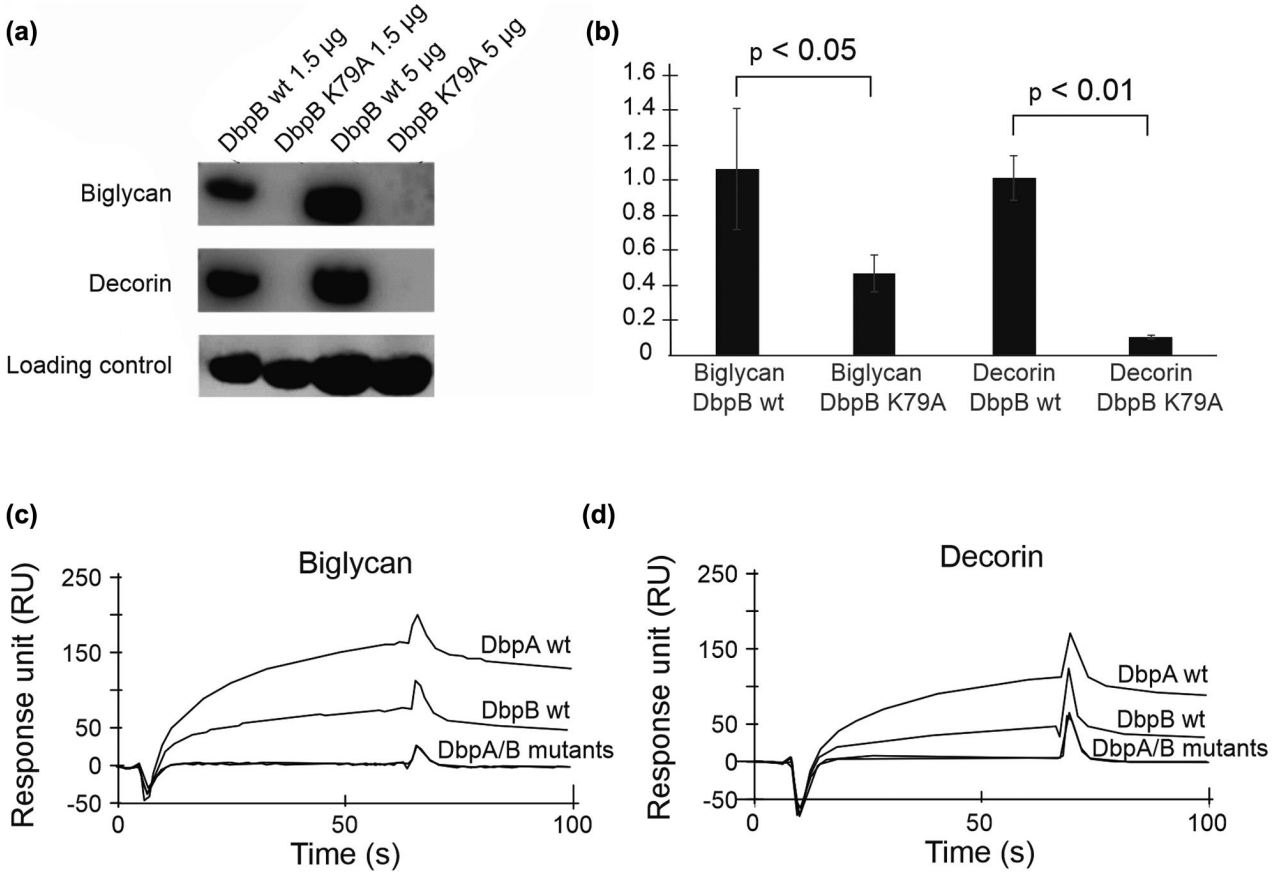

FIGURE 4 Binding of recombinant Dbps to biglycan and decorin. (a) Varying amounts (1.5 µg and 5 µg) of recombinant wild-type (wt) DbpB and K79A DbpB were run on a gel and blotted. Biotinylated decorin or biglycan were incubated with the membranes and bound proteoglycans were detected with horseradish peroxidase labeled streptavidin. As a loading control, a protein gel was dyed with SimplyBlue safe stain. (b) Wt and mutated DbpB proteins were coated on a microtiter plate. Biotinylated decorin or biglycan were added to the wells and bound proteoglycans were detected with alkaline phosphatase-conjugated streptavidin. The data are expressed as OD 405 nm values ± standard deviations subtracted with the OD 405 nm values of the control wells. (c and d) In surface plasmon resonance studies, CM5 chips were coated with Dbps (50 µg/ml) and 1 µM of biglycan (c) or 1 µM of decorin (d) were run through the flow cells. The data are expressed as response units

JF105 strains were allowed to interact with HBMECs grown on microtiter plate wells. Unbound bacteria were washed away and the adhered carboxyfluorescein diacetate succinimidyl ester (CFSE)-labeled Lyme borreliae were visualized with a microscope. JF105 transformed with pME22 plasmid only served as a negative control and showed only modest binding to the cells (Figure 6d). The strain expressing wt Dbps bound to the cells significantly more than the background strain ($p < .001$). JF105 strain expressing mutated Dbps, on the contrary, bound to the cells significantly less ($p < .001$) than the strain expressing wt Dbps and exhibited only background level binding.

3 | DISCUSSION

Dbps are important virulence determinants for Lyme borreliae. They are expressed in a mammalian host, and strains lacking the Dbps are dissemination defective in the mouse model of LB (Imai et al., 2013). In addition, Dbps are required for the development of joint manifestations (Salo et al., 2015). One striking feature of Dbps is that, depending on the Lyme borreliae genospecies, the proteins bind proteoglycans and glycosaminoglycans with different affinities, which seems to have an effect on the tissue tropism of the spirochetes (Benoit et al., 2011; Lin et al., 2014; Salo et al., 2011, 2016). The Dbps have been shown to have lysine residues that are important in binding to decorin and glycosaminoglycans (Brown et al., 1999; Feng & Wang, 2015; Fortune et al., 2014; Morgan & Wang, 2015; Pikas et al., 2003; Wang, 2012).

In this study, we show that DbpA and DbpB of Bg SBK40 also carry these critical lysine residues. K80 in DbpA and K79 in DbpB are conserved among all published sequences of Bg, which strongly indicates their importance in the Dbp proteins. K78 and K82 of DbpA, on the contrary, which are part of a second potential binding site, are only conserved in some of the strains and are substituted for aspartate, glutamate, arginine, or glutamine in most of the nonconserved strains (Supplementary Figure S1). Arginine is positively charged and can form even stronger ionic interactions than lysine (Gandhi & Mancera, 2008). Glutamate,

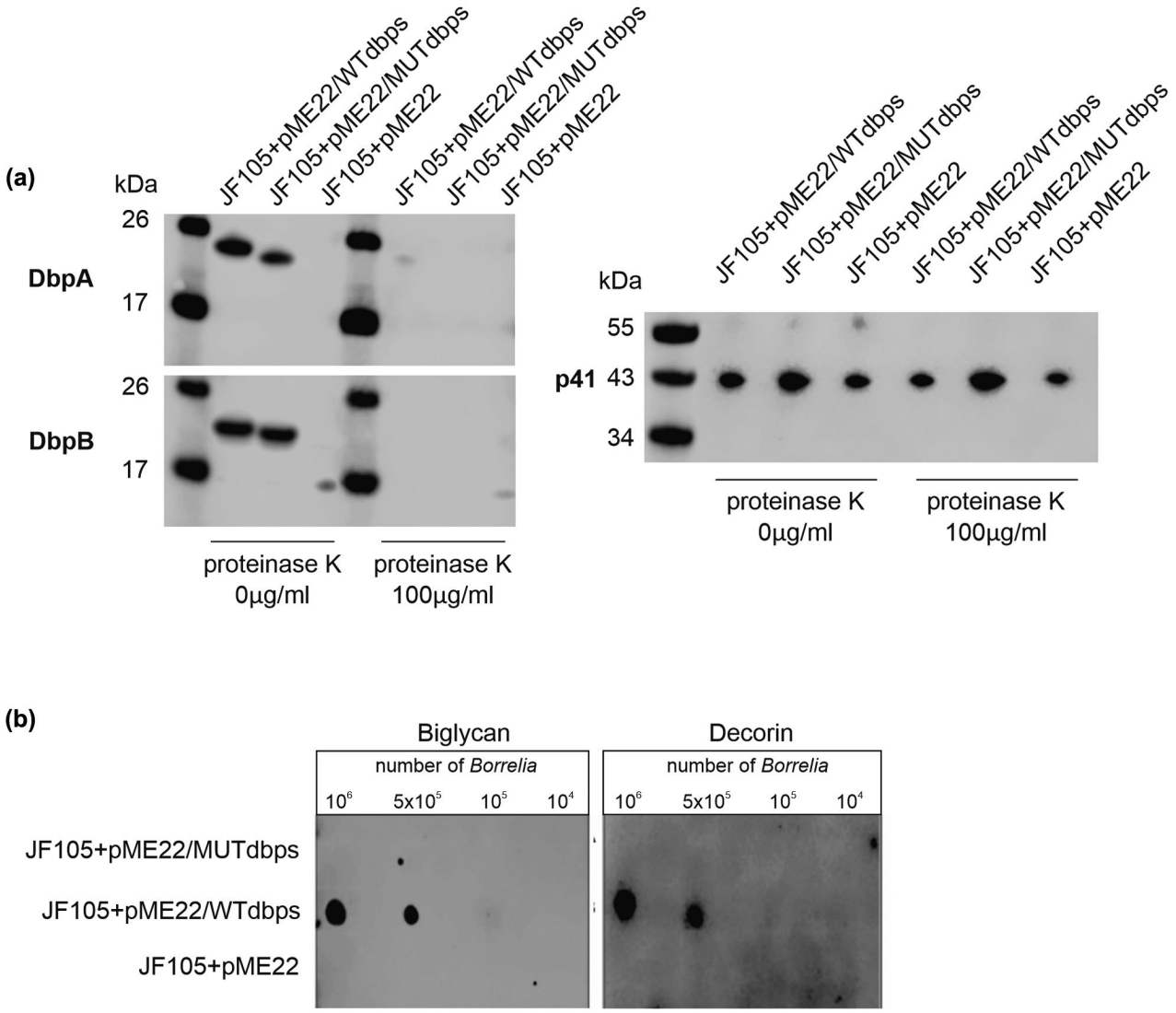

FIGURE 5 The surface localization of Dbps and binding of Bbss JF105 strains to biglycan and decorin. (a) The expression of Dbps on the surface of Bbss JF105 was detected with Western blot. Bacteria were incubated either without proteinase K (0 µg/ml) or with proteinase K (100 µg/ml) and loaded on 10% NuPAGE Bis-Tris protein gels and blotted on a nitrocellulose membrane. The membrane was incubated with rabbit-anti-DbpA/BgSBK40 or rabbit-anti-DbpB/BgSBK40 immune serum or as a loading control with rabbit-anti flagellin antibody. Bound antibodies were detected with horseradish peroxidase-conjugated goat anti-rabbit IgG. (b) JF105 strains were allowed to adhere to nitrocellulose membrane. After blocking, the membrane was incubated with biotinylated decorin or biotinylated biglycan. Bound proteoglycans were detected with horseradish peroxidase-conjugated streptavidin

aspartate, and glutamine are, however, not positively charged and cannot form ionic interactions with the negatively charged GAGs. However, GAGs can also interact through hydrogen bonds (Gandhi & Mancera, 2008), and thus, the interactions with the GAGs could likely be maintained to some degree despite these residue differences. Another possibility is that the second GAG-binding site formed by these residues is not found in all Dbps but is instead compensated for by residues in other positions, as it has been shown that Dbps can have several binding sites that are uniquely adapted to each protein (Feng & Wang, 2015; Morgan et al., 2015; Morgan & Wang, 2015).

When K78/80/82 in DbpA and K79 in DbpB are mutated to alanine, the resulting recombinant proteins almost completely lose their ability to bind decorin and biglycan as demonstrated by Western blot, microtiter plate assay, and a flow-based Biacore assay. The binding of wt and mutated recombinant DbpA was analyzed only with a flow-based method since we have previously shown that wt DbpA of Bg SBK40 is able to bind proteoglycans only under flow conditions (Salo et al., 2016). These results show that the mutated lysine residues of both DbpA and DbpB play a role in GAG-binding. As GAGs bind mainly through electrostatic interactions, the loss of surface charge in the mutants, as shown by the electrostatic surface potential maps (Figure 3), can explain the reduced GAG-binding seen in the mutants.

Thermofluor analysis was performed to analyze the folding and stability of the mutated proteins in comparison with the wt proteins.

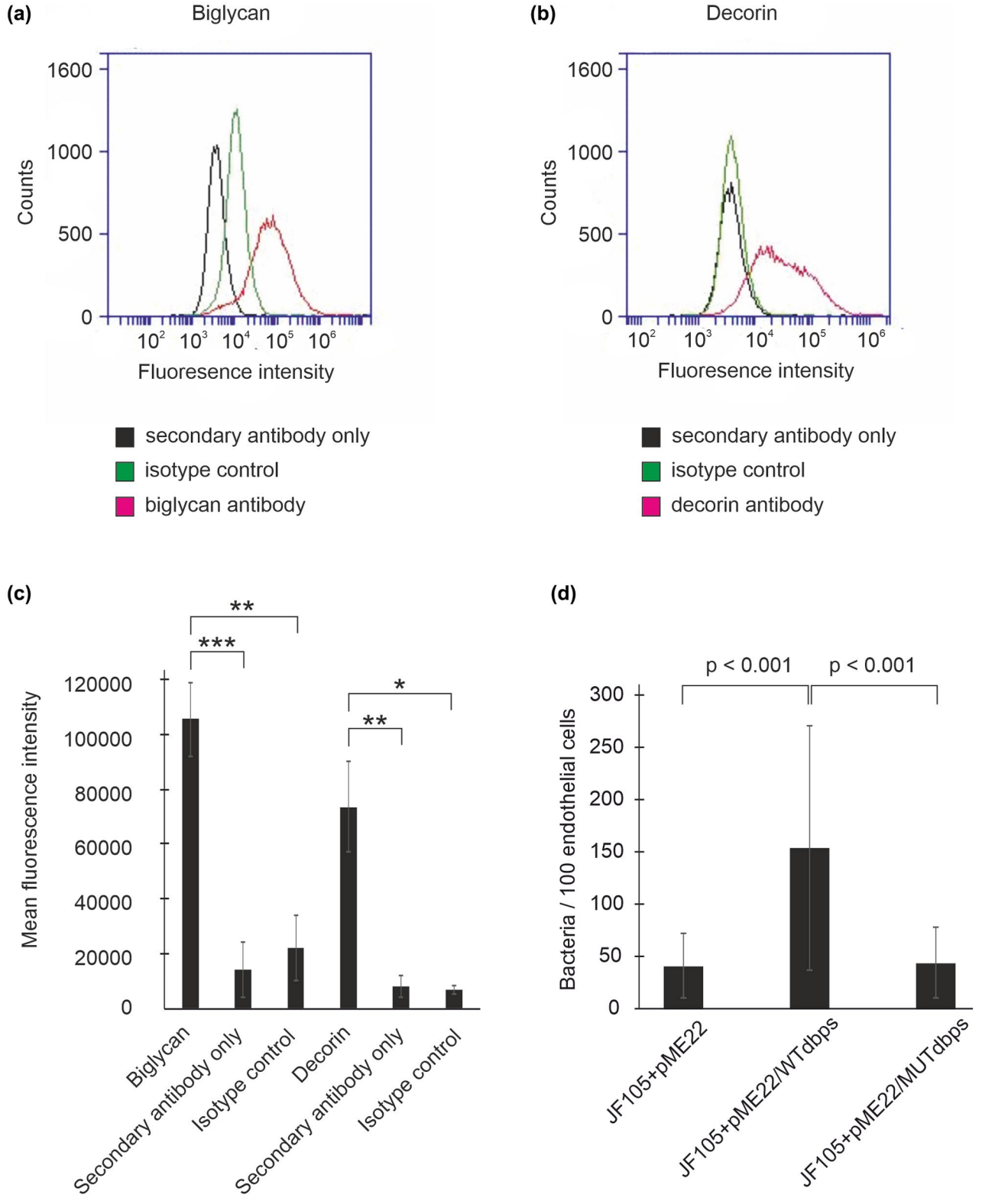

FIGURE 6 The expression of biglycan and decorin in HBMECs and the binding of JF105 strains to the cells. Proteoglycan expression was detected with flow cytometry by using monoclonal biglycan antibody clone 4E1-1G7 (a) or monoclonal decorin antibody clone 9XX (b). Mouse IgG1 and mouse IgG2a κ clone were used as isotype control antibodies, respectively. Goat anti-mouse IgG Alexa Fluor 488 was used as a secondary antibody. Also, as a control, samples treated with the secondary antibody only were analyzed. The fluorescence was detected using Accuri C6. (c) Mean fluorescence intensities were determined with C6 software and a *t* test was used for statistical analyses. The data are expressed as mean fluorescence intensity of three independent samples ± standard deviation. $^*p < .05$, $^{**}p < .01$, $^{***}p < .001$. (d) HBMECs were grown on 96-well plates for 3 to 4 days. 50×10^6 carboxyfluorescein diacetate succinimidyl ester (CFSE) labeled bacteria were allowed to adhere to the cells at RT for 1 hr. Unbound bacteria were washed, and the wells were imaged with EVOS FL Auto 2 Cell Imaging System. Bound bacteria were calculated in ImageJ and the data were analyzed with Kruskal–Wallis test (corrected with Steel-Dwass post hoc test) with JMP Pro 14. The data are expressed as bacteria/100 cells in three independent experiments ± standard deviation

In this method, the protein is denatured in the presence of a dye, which binds to the gradually exposed hydrophobic parts of the protein. By binding to the protein, the dye becomes fluorescent, which can be monitored. The analysis revealed that the melting temperature (Tm) of mutated DbpA was ca 7°C lower than that of the wt protein. This implicates that the mutant DbpA is not as stable as the wt protein. However, we assumed that the folding of the mutated protein was not dramatically altered since the difference between the Tm values was rather modest. We performed MD-simulations for the 3D models of wt and mutant Dbps, which showed that they remained stable throughout the simulation, indicating that the mutations do not affect the 3D fold of the protein. We were also able to show that mutated DbpA was expressed on the surface of Lyme borreliae, supporting our assumption that the tertiary structure of the mutated protein was intact. Furthermore, others have demonstrated that point mutations from lysine to alanine have not altered the tertiary structure of other Dbps (Brown et al., 1999; Fortune et al., 2014).

It has been shown by Morgan and Wang (Morgan & Wang, 2015) that DbpA of Bg Pbr has two GAG binding sites. In DbpA of Bg Pbr, K79 is facing the binding pocket but K77 and K81 are facing to the opposite direction and form a second binding site together with two other lysine residues (K173 and K176). They also showed that these two binding sites act independently of each other. The three lysines 77/79/81 in DbpA of Bg PBr align with K78/K80/K82 in DbpA of Bg SBK40, and the homology model we created for DbpA of Bg SBK40 shows that K80 is located in the canonical binding pocket while K78 and K82 point to the opposite side and potentially form a second binding site. K173 and K176, shown to be important for GAG-binding in Bg PBr, correspond to K174 and E177 in Bg SBK40 DbpA. K174 can contribute to the GAG-binding together with K78 and K82, while the negatively charged E177 will not be able to form similar ionic interactions with GAG chains.

To study the importance of the two binding sites in DbpA, a triple mutant K78/80/82A was created. By mutating only K80, which is totally conserved in all studied Dbp sequences and crucial for GAG-binding (Brown et al., 1999), the GAG-binding might still have been mediated through the potential second binding site, consisting of K78, K80, and K174. The corresponding second binding site in Bg PBr DbpA has been shown to have the same affinity for GAGs as that of the canonical binding site (Morgan & Wang, 2015). Thus, by mutating residues from both binding sites we ensured that we had a nonfunctional protein suitable for performing a comprehensive study of the role of Dbps of *B. garinii* in adherence to HBMECs. According to Morgan and Wang (Morgan & Wang, 2015), K173/K176 are more important in the second binding site than K77/K81. However, our results show that the mutated recombinant DbpA (K78/80/82A), still containing the intact K174, did not bind proteoglycans at all in the Biacore experiment and the Lyme borreliae strain expressing K78/80/82A mutations in DbpA and K79A in DbpB bound HBMECs as weakly as the background strain with no Dbps. This indicates that K174 does not significantly mediate binding of Bg SBK40 DbpA to proteoglycans/HBMECs and, thus, we can conclude that our strategy of mutating all three lysines 78, 80, and 82 was suitable for identifying the residues critical for DbpA adhesion to HBMECs.

DbpB of Bbss B31 also has multiple GAG binding sites (Feng & Wang, 2015). Of these, the canonical binding site is only secondary while the long unstructured C-terminal tail of the protein is the primary GAG binding site. However, when we mutated only one amino acid (K79) located in the canonical binding site in DbpB of Bg SBK40, we could not detect any binding to either of the studied proteoglycans in Biacore or Western blot analysis and only weak binding to biglycan in the microtiter plate assay. Thus, in contrast to DbpB of Bbss B31, it seems that in DbpB of Bg SBK40, the canonical binding site plays a crucial role in the binding of proteoglycans. Further, the C-terminal tail seems not to be the primary proteoglycan binding domain even though, according to the amino acid sequence and the predicted structure, DbpB of Bg SBK40 has a long unstructured C-terminal tail rich in lysine residues like DbpB of Bbss B31. Three lysines and one asparagine are the last residues in the C-terminal tail of Bg SBK40 DbpB, whereas the corresponding residues in Bbss B31 DbpB are all lysines. As asparagine is not a positively charged residue that could form ionic interactions with the GAGs, this difference might contribute to the reduced importance of the C-terminal tail as a GAG-binding site in Bg SBK40 DbpB. Moreover, the canonical GAG-binding site in Bbss B31 consist of two lysines and one glutamine (Feng & Wang, 2015). Since glutamine is also a noncharged residue this further suggests that the lysine-rich C-terminal tail of Bbss B31 DbpB can compensate for the missing lysine in the canonical binding site. In Bg SBK40 DbpB, the canonical GAG-binding residues are two lysines and an arginine (K79, K160 and R167). However, as arginines have been shown to bind more strongly than lysines to GAGs (Gandhi & Mancera, 2008; Hileman et al., 1998), R167 should not reduce GAG-binding, instead it could enhance the importance of the canonical GAG-binding site in DbpB of Bg SBK40.

Our MD-simulations showed that the linker is more flexible in wt DbpB than in the mutant (Supplementary Figure S3c). In the mutant DbpB, the smaller size and the hydrophobic nature of A79 compared to K79 allows the linker to extend further down toward the canonical binding site. Morgan *et al*. have shown that the shape of the linker impacts the GAG-binding affinity of DbpAs (Morgan et al., 2015) and a more compact shape, like the helical linker in Bg SBK40 DbpA, gives a more exposed binding pocket and increases the binding affinity. The DbpB mutant linker, which can reach further down toward the binding site, might, therefore, in a similar manner partly cover the binding site. The MD-simulation also showed that the backbone residues near K79/A79 are slightly more flexible in the mutant. K79 in wt DbpB forms hydrogen bonds and electrostatic interactions with the surrounding residues and its position is, therefore, more fixed by these interactions, whereas A79 in mutant DbpB lacks these interactions and, thus, confers flexibility.

Bg is the most common cause of neuroborreliosis in Europe and it is thought to spread from the initial tick feeding site in the skin to the central nervous system via the blood circulation (Moriarty et al., 2008; Stanek & Strle, 2018). To reach the central nervous

system, Lyme borreliae must first spread via the vasculature, adhere to HBMECs, and traverse across the blood–brain barrier. The adherence of Lyme borreliae to various endothelial cells like human umbilical vein endothelial cells has been studied before (Coburn et al., 2013; Leong et al., 1998; Salo et al., 2016). Interestingly, it has been demonstrated at protein level that DbpA of *B. bavariensis* is able to interact with HBMECs (Tkáčová et al., 2020). In the dura mater of mice, Lyme borreliae are associated with the vascular regions (Divan et al., 2018), but to our knowledge, there are no previous studies on the adhesion of Lyme borreliae to vascular endothelial cells originating from human brain.

In this study, we constructed JF105 Lyme borreliae strains expressing the wt or the mutated Dbps of Bg SBK40 on their surface to study the role of Dbps and the lysines in endothelial adhesion. Loss-of-function JF105 strain was used as the background in cloning because we wanted to evaluate whether the Dbps are important in binding to HBMECs when they are expressed on an infectious strain. This strategy results in more wt-like bacteria than the strategy of using a noninfectious background strain. By using a loss-of-function strain, we were also able to evaluate the role of Dbps in relation to other functionally redundant adhesins expressed on Lyme borreliae which also might contribute to HBMEC binding. In accordance with this strategy, we show that the Dbps of Bg SBK40 are able to mediate adherence to HBMECs. Lyme borreliae strain lacking Dbps bound significantly less to the cells than the strain expressing wt Dbps. These differences were observed even though JF105 strain most likely expresses redundant adhesins shown to be involved in binding to GAGs and endothelial cells (e.g., BBK32 (Fischer et al., 2006)). On the contrary, the use of a loss-of-function background strain that expresses other adhesins on its surface might explain why also the strain without Dbps bound HBMECs to some extent. Redundant adhesins might also, in part, account for the relatively high variance seen in the binding experiments. To conclude, by using the loss-of-function background instead of cloning the adhesins into a noninfectious gain-of-function background (e.g., *B. burgdorferi* B313), we were able to demonstrate the critical role of Dbps in HBMEC binding since other adhesins, despite their possible redundant roles, did not hide the binding effect of Dbps.

Previously, we have not been able to detect expression of decorin neither in human umbilical vein endothelial cells nor in endothelial cells of skin, heart, and brain tissues (Salo et al., 2016). In contrast, according to flow cytometry analysis, HBMECs clearly expressed both biglycan and decorin and, thus, both of these proteoglycans in HBMECs most likely act as ligands for Dbps. We were also able to demonstrate that, in addition to being important in recombinant proteins, the lysine residues in Dbps are also important when the proteins are expressed on Lyme borreliae. JF105 strain expressing the Dbps with lysine to alanine point mutations showed only background level binding to the HBMECs. These results indicate that the Dbps (and the lysine residues) most likely have a role in the pathogenesis of neuroborreliosis. Of note, Lyme borreliae have been shown to infect the dura mater of mice where decorin is highly expressed (Casselli et al., 2020).

The role of DbpA and/or DbpB of Bbss N40 in binding to another neuronal cell line (C6 glial cells) has been studied before by using a gain-of-function strain as a background in cloning (Fischer et al., 2003). It was shown that DbpB, but not DbpA, is able to bind C6 glial cells. DbpA versus DbpB of Bbss N40 exhibit different GAG-binding properties which is considered to account for the differences seen in cell adhesion. In addition, Dbps of N40 were not able to mediate adherence to EAhy-926 endothelial cells. In our study, we showed that when both DbpA and B of Bg SBK40 are expressed on a loss-of-function background strain, binding to HBMECs is more efficient than binding of a strain that does not express Dbps. Thus, Dbps of different genospecies and strains, indeed, seem to account for the tissue tropism. Previously, we have shown that Dbps of Bg SBK40 act in a flow tolerant manner which is an important feature for adhesins during hematogenous dissemination and supports our hypothesis that Dbps of Bg have a role in the pathogenesis of neuroborreliosis also in vivo (Salo et al., 2016). The Dbps used in this study originate from Bg SBK40 strain which has been isolated from the human skin. However, since there is no mouse model for neuroborreliosis, the role of Dbps of Bg SBK40 in neuroborreliosis in vivo remains to be confirmed.

As a conclusion, we demonstrate that the lysine residues in the canonical binding pockets of Dbps of Bg are crucial for binding to biglycan and decorin. We also show that these lysines are conserved among different Bg strains, underlining their importance in the function of the Dbps. Importantly, Dbps and the lysines contribute to binding of Lyme borreliae to HBMECs and are, thus, potentially critical factors in the pathogenesis of neuroborreliosis.

4 | EXPERIMENTAL PROCEDURES

4.1 | Bacterial strains and human brain microvascular endothelial cells

Escherichia coli strain M15 (Qiagen, Hilden, Germany) was used for cloning and expression of Dbps (Heikkilä et al., 2002a, 2002b). *E. coli* DH5α was used to purify pME22 plasmid containing the *dbpBA* operon of *B. garinii* SBK40 (infectious strain both in mice and men (Cuellar et al., 2019; Heikkilä et al., 2002b)). *E. coli* XL10-Gold (Agilent, Santa Clara, CA) was used in cloning of site-directed mutants. All *E. coli* strains were cultured in Luria Bertani broth or agar with appropriate antibiotics at 37°C overnight. Lyme borreliae strain JF105 (Bbss B31 missing linear plasmid 25, Δ*dbpBA*; loss-of-function strain) used in the study was a kind gift from Assistant Professor Yi-Pin Lin (State University of New York at Albany, Albany, NY) and has been described elsewhere (Lin et al., 2014; Weening et al., 2008). All Lyme borreliae strains were cultured in Barbour–Stoenner–Kelly II (BSK II) broth at 33°C. All experiments were performed when the bacteria were at a logarithmic growth phase. The growth phase and the number of Lyme borreliae was studied using a Neubauer counting chamber.

HBMECs have been described elsewhere (Kamiichi et al., 2012). Briefly, the cells were grown on collagen coated flasks or plates in Complete Medium with serum (Cell systems, Kirkland, WA) supplemented with CultureBoost-R (Cell systems), penicillin–streptomycin (Sigma, Steinheim, Germany) and 4 μg/ml blasticidin S (Sigma) with 5% CO_2 at 33°C. The experiments were performed with cells grown for 3 to 4 days.

4.2 | Sequence alignments, homology modeling, and MD-simulations

To find suitable structural templates for creating homology models, BLAST (Basic Local Alignment Search Tool) (Altschul et al., 1990) searches against the pdb database were made with the Bg SBK40 DbpA (UniProt code Q8VVC2) and DbpB (UniProt code Q8RJE3) sequences as queries. Five structures with acceptable E-values (E-values < 0.001 are statistically significant (Pearson, 2013)) were found, Bg PBr DbpA (PDB ID: 2mtd, (Morgan & Wang, 2015)), Bbss DbpA (PDB ID: 4onr, (Fortune et al., 2014)), Bbss DbpB (PDB ID: 2mvg, (Feng & Wang, 2015)), Bbss B31 DbpA (PDB ID: 2lqu, (Wang, 2012)), and Bbss N40 DbpA (PDB ID: 2mtc, (Morgan & Wang, 2015)). A structure-based alignment was made with these structures using VERTAA in Bodil (Johnson & Lehtonen, 2000). The Bg SBK40 DbpA and DbpB sequences were aligned to the prealigned structure-based alignment and models were created with Modeller (Sali & Blundell, 1993) based on the alignment. The structures with the highest sequence identities to the Dbps were used as the structural templates, DbpA was modeled on the Bg PBr DbpA (2mtd) structure and DbpB on the Bbss DbpB (2mvg) structure. Separate models were also created with the mutations DbpA K78A/K80A/K82A and DbpB K79A. The models were evaluated by ModFOLD (Maghrabi & McGuffin, 2017) and ProQ (Wallner & Elofsson, 2003). PyMOL (The PyMOL Molecular Graphics System, Version 2.0.6 Schrödinger, LLC) was used for analyses, visualization and for preparing figures. The alignment figure was prepared using ESPript 3.0 (Robert & Gouet, 2014).

Molecular dynamics (MD) simulations of the Dbp models were done with Desmond Molecular Dynamics System (2019-4) in Maestro (Bowers et al., 2006). The proteins (DbpA, DbpA-A78/A80/A82, DbpB, and DbpB-A79) were solvated using a TIP3P water model (Jorgensen et al., 1983) in an octahedral box with 20 Å distance between the solute surface atoms and the edge of the box. The systems were neutralized by addition of Cl^- atoms. The OPLS3e force field (Harder et al., 2016) was used, with a constant temperature of 300 K and constant pressure (1.01325 bar) that were respectively maintained with the Nosé–Hoover chain thermostat and the Martyna-Tobias-Klein barostat. The systems were relaxed with the default equilibration protocol in Desmond and the simulations were run for 200 ns. The resulting trajectories were analyzed using the Simulation Interactions Diagram program in Desmond. All simulations were done in triplicate with randomized initial velocities.

4.3 | Construction of mutated recombinant proteins

Lysines 78/80/82 in DbpA of Bg SBK40 and lysine 79 in DbpB of Bg SBK40 were mutated to alanine with site-directed mutagenesis. Wild-type (wt) Dbp-proteins of Bg SBK40 cloned into pQE30 expression vector of *E. coli* are described elsewhere (Heikkilä et al., 2002a, 2002b). The expression plasmids were purified from *E. coli* M15 with QIAprep Spin Miniprep Kit (Qiagen) according to the manufacturer's instructions. Purified plasmids were used as templates in the mutagenesis reactions. Mutations were prepared with QuikChange II Site-Directed Mutagenesis kit (Agilent) according to the manufacturer's instructions with primers listed in Supplementary Table S2. Mutations were verified by sequencing the *dbp*-genes. Resulting plasmids containing the mutations were then transformed back into *E. coli* M15. Recombinant proteins were induced and purified as described elsewhere (Salo et al., 2011) and the protein concentrations were analyzed with BCA-kit (Pierce, Thermo Fisher Scientific, Waltham, MA) according to the manufacturers' instructions.

4.4 | Thermofluor analysis

The proteins were diluted to the concentration of 1 mg/ml and mixed 1:1 with Sypro Orange protein dye (Sigma) dilution (1:55). Total of 5 μl of the mixture was added on the polymerase chain reaction plate with 20 μl of PBS. We used triplicate as well as controls with no protein. The measurements were carried out using Light Cycler 480 II equipment (Roche Life Science, Mannheim, Germany). In the protocol, the temperature was raised step by step from 20°C to 99°C. For the analysis, the data were exported, the average of three triplicate wells was determined for each data point, the reference value subtracted, and the curves were visualized. The melting temperature (Tm) was determined as temperature where 50% of protein was denatured.

4.5 | Binding of DbpB proteins to decorin and biglycan under stationary conditions

Binding of wt DbpB and mutated DbpB/K79A to decorin and biglycan was studied under stationary conditions with Western blot and in a microtiter plate assay.

For Western blot analysis, DbpB proteins were loaded on 10% Bis-Tris gels (NuPAGE, Thermo Fisher Scientific) and run in MES buffer (Novex, Thermo Fisher Scientific). Then, the proteins were blotted on a 0.2 μm nitrocellulose membrane (Whatman, GE Healthcare, Chicago, IL) and blocked with 3% skim milk in tris-buffered saline with 0.05% Tween20 (TBST) at RT for 2 hr after which the blocking solution was removed by rinsing the membrane with TBST. Biotinylated decorin or biotinylated biglycan (10 μg/ml, biotinylated with EZ-Link NHS-LC-Biotin (Pierce, Thermo Fisher Scientific) according to manufacturer's instructions) was then incubated with the membrane at 4°C overnight. Unbound

proteoglycans were removed by washing the membranes three times with TBST. Bound proteoglycans were detected by incubating streptavidin-horseradish peroxidase (HRP; 0.5 μg/ml, Pierce, Thermo Fisher Scientific) with the membranes at RT for 1 hr. Unbound streptavidin was removed by washing the membranes three times with TBST and the bound streptavidin-HRP was detected with WesternBright ECL HRP substrate (Advansta, San Jose, CA) and Odyssey Fc imaging system (Licor Biotechnology, Bad Homburg, Germany). As a loading control, one SDS-PAGE gel loaded with Dbps was stained with SimplyBlue safe stain (Thermo Fisher Scientific) and imaged with Odyssey Licor Fc.

For the microtiter plate assay, purified Dbps were coated on enhanced binding microtiter plates (Thermo Fisher Scientific) 10 μg/ml in PBS for 1 hr at 37°C after which the wells were blocked with 1% BSA in PBS at 37°C for 1 hr. A 100 nM of biotinylated decorin and biglycan were added to the wells in PBS + 0.05% Tween 20 (PBST) and incubated at 37°C for 1 hr. As a control, two wells were incubated with PBST only. Unbound proteoglycans were removed by washing the wells three times with TBST. Bound proteoglycans were detected by incubating 1 μg/ml of alkaline phosphatase-conjugated streptavidin (Pierce, Thermo Fisher Scientific) in TBST in the wells at 37°C for 1 hr. Unbound streptavidin was removed by washing the wells three times with TBST and bound streptavidin was detected by incubating p-NPP-Na_2 substrate (1 mg/ml; Reagena, Toivala, Finland) on the wells for 20 min before the reaction was stopped with 1 M sodium hydroxide. The absorbances (OD 405 nm) were measured with a Multiskan EX spectrophotometer (Thermo Fisher Scientific). The results are expressed as the OD 405 nm values subtracted with the OD 405 nm values of the control wells (wells without biotinylated proteoglycans). Statistical differences in binding of proteoglycans between wt DbpB and mutated DbpB/K79A were analyzed with a *t* test.

4.6 | Binding of Dbps to decorin and biglycan under flow

Binding of Dbps to decorin and biglycan under flow was studied with surface plasmon resonance assay using Biacore X (GE Healthcare) as described elsewhere (Salo et al., 2016). Briefly, Dbps (50 μg/ml in 10 mM sodium acetate buffer pH 5) were immobilized on CM5 sensor chips (GE Healthcare) by amine coupling (5 μl/min). The empty reference flow cells were treated with the same buffer as the coated flow cells but without Dbps. Final immobilized level of each Dbp as response units (RU) were calculated as RU of the flow cell subtracted with RU of the blank reference flow cell (1,248 RU for DbpA wt, 1,179 RU for DbpA/K78/80/82A, 1,229 RU for DbpB wt, and 1,102 RU for DbpB/K79A). Decorin and biglycan were diluted to HBS-P running buffer (10 mM HEPES pH 7.4, 0.15 M NaCl, 0.005% (v/v) Surfactant P20) at concentrations of 1 μM and injected to the flow cells 10 μl/min. BSA (1 μM) was used as a negative control ligand. The data were analyzed using BIAevaluation software version 4.1 (GE Healthcare).

4.7 | Construction of point mutations to pME22 expression plasmid

The pME22 plasmid containing the *dbpBA* operon of Bg SBK40 (pME22/WTdbps) was purified from *E. coli* DH5α with QIAprep Spin Miniprep Kit (Qiagen) and used as a template in the mutagenesis reaction for DbpA. Lysines 78/80/82 in DbpA were mutated to alanine with QuikChange II XL Site-Directed Mutagenesis kit (Agilent) with the primers listed in Supplementary Table S2 as instructed by the manufacturer with the following modifications: the amount of template used for the reactions was 200 ng and QuikSolution was not included. The elongation step in the cycling protocol was 2.5 min per kb of plasmid. After the cycling, Dpn I digestion was performed as instructed to destroy the template DNA. The resulting DNA created by PCR was precipitated with EtOH and transformed into *E. coli* XL10-Gold as instructed. Pure cultures of colonies were sequenced to verify that the mutations had occurred to right places and that no other additional mutations to the *dbpBA* operon had occurred. One clone with mutations K78/80/82A in *dbpA* sequence was chosen for further mutation steps. Mutated pME22 plasmid (K78/80/82A in *dbpA*) was purified and used as a template to construct *dbpB* mutation to the same plasmid. K79A mutation to *dbpB* was performed as the mutations to *dbpA*. Again, plasmid preparations of pure cultures of the resulting transformants were sequenced to verify that the *dbpBA* operon in pME22 contained the mutations K78/80/82A in *dbpA* and K79A in *dbpB* and that no other mutations to the operon had occurred. One clone was chosen for further experiments and the resulting mutated plasmid was named pME22/MUTdbps.

4.8 | Transformation of Lyme borreliae strains

The plasmids pME22, pME22/WTdbps, and pME22/MUTdbps were extracted and purified with Plasmid Midi kit (Qiagen) from *E. coli* according to the manufacturer's protocol. 1×10^9 JF105 bacteria were centrifuged at 1,500*g* and washed with ice-cold electroporation buffer (0.27 M sucrose and 15% (v/v) glycerol) three times. Then, about 30 μg of DNA was electroporated into JF105 with 2.5 kV, 200 Ω, and 25 μFa. After incubating the transformed JF105 in BSK II without antibiotics at 33°C overnight, 300 μg/ml kanamycin and 50 μg/ml gentamycin were added to the medium. The transformed bacteria were maintained in 96-microtiter plates (200 μl/well) at 35°C with 5% CO_2. The resulting colonies were inoculated into 6 ml of fresh BSK II with 300 μg/ml kanamycin and 50 μg/ml gentamycin.

4.9 | Plasmid profiling

The plasmid profiles of the transformed Lyme borreliae strains were assessed by multiplex PCR (Bunikis et al., 2011). The DNA of the transformed Lyme borreliae strains and their parent strain was extracted with High Pure PCR Template Preparation kit (Roche Life Science) according to the manufacturer's protocol. Then, the circular and linear plasmids

were amplified as described. The plasmids were stained with Midori green dye (Nippon Genetics, Düren, Germany) on 2.5% agarose gel.

4.10 | Immunodetection

The expression of wt and mutated DbpA and DbpB, and flagellin (p41) was detected with Western blot. 50×10^6 bacteria were collected by centrifugation and resuspended in 75 μl of water and 25 μl of 40× NuPAGE Sample Buffer (Life Technologies). Samples were loaded to 10% NuPAGE Bis-Tris protein gels (Thermo Fisher Scientific) and electrophoresis was run with MES-buffer (Thermo Fisher Scientific) at 200 V for 1 hr. The proteins were blotted as described above and blocked with 5% skim milk in PBS at 4°C overnight. The membrane was incubated with rabbit-anti-DbpA/BgSBK40 or rabbit-anti-DbpB/BgSBK40 immune serum (MedProbe/BioNordika, Oslo, Norway) in 5% skim milk in PBST at 4°C overnight or rabbit-anti flagellin antibody (1:1,000; Aviva Systems Biology, San Diego, CA) in 5% skim milk in PBST at RT for 1 hr. After washing the membrane three times with PBST, the membrane was incubated with HRP-conjugated goat anti-rabbit IgG (1:5,000; Santa Cruz Biotechnologies, Santa Cruz, CA) in PBST at RT for 1 hr. After washing, the proteins were imaged as described above.

4.11 | Proteinase K-assay

JF105 bacteria were washed with PBS containing 5 mM $MgCl_2$, diluted to 1×10^8 bacteria/ml, and incubated with 0 or 100 μg/ml proteinase K (Sigma) at RT for hour. The bacteria were washed with the aforementioned buffer before analyzing the bacterial lysate samples by Western blot as described above.

4.12 | Dot blot -binding assay

Spots of 1 μl containing 10^6, 5×10^5, 10^5, or 10^4 of JF105 + pME22/MUTdbps, JF105 + pME22/WTdbps, and JF105 + pME22 bacteria were allowed to adhere to nitrocellulose membrane (Protran BA 85, Whatman, GE Healthcare). The membrane was then blocked with 3% skim milk in TBST at 4°C overnight. After blocking, the membrane was incubated with biotinylated decorin (Pierce, Thermo Fisher Scientific; 2 μg/ml) or biotinylated biglycan (Pierce, Thermo Fisher Scientific; 4 μg/ml) in TBST at RT for 1 hr. After washing the membrane with TBST, the membrane was incubated with HRP-conjugated streptavidin (Pierce, Thermo Fisher Scientific; 0.1 μg/ml) in TBST at RT for 1 hr and was imaged as described above.

4.13 | Flow cytometry

The expression of biglycan and decorin was detected in HBMECs with flow cytometry. HBMECs were detached from culture dish with 0.1% trypsin-EDTA. The cells were then washed once with serum containing culture medium and fixed at 33°C for 5 min with 4% paraformaldehyde (Santa Cruz Biotechnology). The fixative was removed by washing the cells three times with PBS. Unspecific protein-protein interactions were blocked by treating the cells with 0.1 M glycine in PBS at RT for 5 min. Proteoglycan expression was detected using monoclonal biglycan antibody clone 4E1-1G7 (dilution 10 μg/ml; Abnova, Taipei, Taiwan) or monoclonal decorin antibody clone 9XX (dilution 10 μg/ml; Santa Cruz Biotechnology). Mouse IgG1 (1 μg; Caltag Laboratories, Carlsbad, CA) and mouse IgG2a κ clone eBM2a (1 μg; Thermo Fisher Scientific) were used as isotype control antibodies. Goat anti-mouse IgG Alexa Fluor 488 (1:1,000; Invitrogen, Thermo Fisher Scientific) was used as a secondary antibody. Also, as a control, samples treated with the secondary antibody only were analyzed. The fluorescence was detected using Accuri C6 (BD, Franklin Lakes, NJ). The data were analyzed with C6 software (BD) and a *t* test was used for statistical analyses (IBM SPSS Statistics, Armonk, NY).

4.14 | Adhesion to HBMECs

HBMECs grown on 96-well plates for 3 to 4 days were fixed with cold 200 μl acetone at RT for 15 min. The wells were washed twice with 200 μl of PBST for 10 min. The cell nuclei were stained with 4′,6-diamidino-2-phenylindole (DAPI; Invitrogen, Thermo Fisher Scientific) diluted 1:2,000 in PBS at RT for 5 min (protected from light). The wells were washed with PBS. The F-actin of the cells was fluorescently stained with Alexa Fluor 568 phalloidin (Invitrogen, Thermo Fisher Scientific) diluted 1:40 in PBS at RT for 1 hr and washed as described before. 50×10^6 CFSE (Molecular probes, Eugene, OR) labeled bacteria were allowed to adhere to the cells at RT for 1 hr. The staining procedure of Lyme borreliae with CFSE has been described elsewhere (Tuominen-Gustafsson et al., 2006). The unbound bacteria were washed, and the wells were imaged with EVOS FL Auto 2 Cell Imaging System (Invitrogen, Thermo Fisher Scientific). Bound bacteria were calculated in ImageJ and the data was analyzed with Kruskal-Wallis test (corrected with Steel-Dwass post hoc test) with JMP Pro 14 (SAS, Cary, NY). The data are expressed as *Borrelia*/100 cells.

ACKNOWLEDGMENTS

We thank Joona Räikkä and Tuula Rantasalo for technical assistance. We thank the bioinformatics (J.V. Lehtonen), translational activities and structural biology (FINStruct) infrastructure support from Biocenter Finland and CSC IT Center for Science for computational infrastructure support at the Structural Bioinformatics Laboratory, (SBL) Åbo Akademi University. SBL is part of the NordForsk Nordic POP (Patient Oriented Products), the Solutions for Health strategic area of Åbo Akademi University, and the InFLAMES Flagship program of the Academy of Finland on inflammation, cancer and infection, University of Turku and Åbo Akademi University.

CONFLICT OF INTEREST

The authors report no conflicts of interest.

AUTHOR CONTRIBUTIONS

Design of the study - JH and AP. Acquisition of the data - AP, MÅ, JC, OG, HE, MR, JS, TF, TAS, and JH. Analysis and interpretation of the data - AP, MÅ, JC, TAS, and JH. Writing of the manuscript - AP, MÅ, JC, TAS, and JH. All authors read and approved the final manuscript.

DATA AVAILABILITY STATEMENT

The data that support the findings of this study are available from the corresponding author upon reasonable request.

ORCID

Annukka Pietikäinen https://orcid.org/0000-0003-3554-0683

REFERENCES

Altschul, S.F., Gish, W., Miller, W., Myers, E.W. & Lipman, D.J. (1990) Basic local alignment search tool. *Journal of Molecular Biology*, *215*, 403–410. Available from: https://doi.org/10.1016/S0022-2836(05)80360-2

Benoit, V.M., Fischer, J.R., Lin, Y.P., Parveen, N. & Leong, J.M. (2011) Allelic variation of the Lyme disease spirochete adhesin DbpA influences spirochetal binding to decorin, dermatan sulfate, and mammalian cells. *Infection and Immunity*, *79*, 3501–3509.Available from: https://doi.org/10.1128/IAI.00163-11

Bista, S., Singh, P., Bernard, Q., Yang, X., Hart, T., Lin, Y.P. et al. (2020) A novel laminin-binding protein mediates microbial-endothelial cell interactions and facilitates dissemination of lyme disease pathogens. *Journal of Infectious Diseases*, *221*, 1438–1447.Available from: https://doi.org/10.1093/infdis/jiz626

Bowers, K.J., Chow, E., Xu, H., Dror, R.O., Eastwood, M.P., Gregersen, B.A. et al. (2006) Scalable algorithms for molecular dynamics simulations on commodity clusters. In: *Proceedings of the 2006 ACM/IEEE conference on Supercomputing*. : Association for Computing Machinery, p. 43.

Brissette, C.A. & Gaultney, R.A. (2014) That's my story, and I'm sticking to it—An update on *B. burgdorferi* adhesins. *Frontiers in Cellular and Infection Microbiology*, *4*, 41.

Brown, E.L., Guo, B.P., O'Neal, P. & Höök, M. (1999) Adherence of *Borrelia burgdorferi*. Identification of critical lysine residues in DbpA required for decorin binding. *Journal of Biological Chemistry*, *274*, 26272–26278.Available from: https://doi.org/10.1074/jbc.274.37.26272

Bunikis, I., Kutschan-Bunikis, S., Bonde, M. & Bergström, S. (2011) Multiplex PCR as a tool for validating plasmid content of *Borrelia burgdorferi*. *Journal of Microbiological Methods*, *86*, 243–247.Available from: https://doi.org/10.1016/j.mimet.2011.05.004

Casselli, T., Divan, A., Tourand, Y., Pecoraro, H.L. & Brissette, C.A. (2020) A murine model of lyme disease demonstrates that *Borrelia burgdorferi* colonizes the dura mater and induces inflammation in the central nervous system. *bioRxiv*: 2020.2004.2024.060681.

Coburn, J., Leong, J. & Chaconas, G. (2013) Illuminating the roles of the *Borrelia burgdorferi* adhesins. *Trends in Microbiology*, *21*, 372–379. Available from: https://doi.org/10.1016/j.tim.2013.06.005

Coburn, J., Magoun, L., Bodary, S.C. & Leong, J.M. (1998) Integrins alpha(v)beta3 and alpha5beta1 mediate attachment of lyme disease spirochetes to human cells. *Infection and Immunity*, *66*, 1946–1952.

Cuellar, J., Pietikäinen, A., Glader, O., Liljenbäck, H., Söderström, M., Hurme, S. et al. (2019) *Borrelia burgdorferi* infection in biglycan knockout mice. *Journal of Infectious Diseases*, *220*, 116–126.Available from: https://doi.org/10.1093/infdis/jiz050

Divan, A., Casselli, T., Narayanan, S.A., Mukherjee, S., Zawieja, D.C., Watt, J.A. et al. (2018) *Borrelia burgdorferi* adhere to blood vessels in the dura mater and are associated with increased meningeal T cells during murine disseminated borreliosis. *PLoS One*, *13*, e0196893. Available from: https://doi.org/10.1371/journal.pone.0196893

Feng, W. & Wang, X. (2015) Structure of decorin binding protein B from *Borrelia burgdorferi* and its interactions with glycosaminoglycans. *Biochimica et Biophysica Acta*, *1854*, 1823–1832.Available from: https://doi.org/10.1016/j.bbapap.2015.08.003

Fischer, J.R., LeBlanc, K.T. & Leong, J.M. (2006) Fibronectin binding protein BBK32 of the Lyme disease spirochete promotes bacterial attachment to glycosaminoglycans. *Infection and Immunity*, *74*, 435–441.Available from: https://doi.org/10.1128/IAI.74.1.435-441.2006

Fischer, J.R., Parveen, N., Magoun, L. & Leong, J.M. (2003) Decorin-binding proteins A and B confer distinct mammalian cell type-specific attachment by Borrelia burgdorferi, the Lyme disease spirochete. *Proceedings of the National Academy of Sciences of the United States of America*, *100*, 7307–7312.Available from: https://doi.org/10.1073/pnas.1231043100

Fortune, D.E., Lin, Y.P., Deka, R.K., Groshong, A.M., Moore, B.P., Hagman, K.E. et al. (2014) Identification of lysine residues in the *Borrelia burgdorferi* DbpA adhesin required for murine infection. *Infection and Immunity*, *82*, 3186–3198.Available from: https://doi.org/10.1128/IAI.02036-14

França, T.C. (2015) Homology modeling: An important tool for the drug discovery. *Journal of Biomolecular Structure & Dynamics*, *33*, 1780–1793. Available from: https://doi.org/10.1080/07391102.2014.971429

Gandhi, N.S. & Mancera, R.L. (2008) The structure of glycosaminoglycans and their interactions with proteins. *Chemical Biology & Drug Design*, *72*, 455–482.Available from: https://doi.org/10.1111/j.1747-0285.2008.00741.x

Grab, D.J., Nyarko, E., Nikolskaia, O.V., Kim, Y.V. & Dumler, J.S. (2009) Human brain microvascular endothelial cell traversal by *Borrelia burgdorferi* requires calcium signaling. *Clinical Microbiology & Infection*, *15*, 422–426. Available from: https://doi.org/10.1111/j.1469-0691.2009.02869.x

Grab, D.J., Perides, G., Dumler, J.S., Kim, K.J., Park, J., Kim, Y.V. et al. (2005) *Borrelia burgdorferi*, host-derived proteases, and the blood-brain barrier. *Infection and Immunity*, *73*, 1014–1022.Available from: https://doi.org/10.1128/IAI.73.2.1014-1022.2005

Harder, E., Damm, W., Maple, J., Wu, C., Reboul, M., Xiang, J.Y. et al. (2016) OPLS3: A force field providing broad coverage of drug-like small molecules and proteins. *Journal of Chemical Theory and Computation*, *12*, 281–296.

Heikkilä, T., Seppälä, I., Saxen, H., Panelius, J., Peltomaa, M., Huppertz, H.I., et al. (2002a) Cloning of the gene encoding the decorin-binding protein B (DbpB) in *Borrelia burgdorferi* sensu lato and characterisation of the antibody responses to DbpB in Lyme borreliosis. *Journal of Medical Microbiology*, *51*, 641–648.

Heikkilä, T., Seppälä, I., Saxen, H., Panelius, J., Yrjänäinen, H. & Lahdenne, P. (2002b) Species-specific serodiagnosis of Lyme arthritis and neuroborreliosis due to *Borrelia burgdorferi* sensu stricto, *B. afzelii*, and *B. garinii* by using decorin binding protein A. *Journal of Clinical Microbiology*, *40*, 453–460.

Hileman, R.E., Fromm, J.R., Weiler, J.M. & Linhardt, R.J. (1998) Glycosaminoglycan-protein interactions: Definition of consensus sites in glycosaminoglycan binding proteins. *BioEssays*, *20*, 156–167.

Imai, D.M., Samuels, D.S., Feng, S., Hodzic, E., Olsen, K. & Barthold, S.W. (2013) The early dissemination defect attributed to disruption of decorin-binding proteins is abolished in chronic murine lyme borreliosis. *Infection and Immunity*, *81*(5), 1663–1673.

Johnson, M.S. & Lehtonen, J.V. (2000) *Bioinformatics: Sequence, structure and databanks. A practical approach*, Higgins, D. & Taylor, W. (Eds.), (pp. 15–50). New York, NY: Oxford University Press.

Jorgensen, W.L., Chandrasekhar, J., Madura, J.D., Impey, R.W., & Klein, M.L. (1983) Comparison of simple potential functions for simulating liquid water. *The Journal of Chemical Physics*, *79*, 926–935.

Kamiichi, A., Furihata, T., Kishida, S., Ohta, Y., Saito, K., Kawamatsu, S. et al. (2012) Establishment of a new conditionally immortalized cell line from human brain microvascular endothelial cells: A promising tool for human blood-brain barrier studies. *Brain Research*, *1488*, 113–122.

Leong, J.M., Wang, H., Magoun, L., Field, J.A., Morrissey, P.E., Robbins, D. et al. (1998) Different classes of proteoglycans contribute to the attachment of *Borrelia burgdorferi* to cultured endothelial and brain cells. *Infection and Immunity*, *66*, 994–999.

Lin, Y.P., Benoit, V., Yang, X., Martínez-Herranz, R., Pal, U. & Leong, J.M. (2014) Strain-specific variation of the decorin-binding adhesin DbpA influences the tissue tropism of the lyme disease spirochete. *PLoS Pathogens*, *10*, e1004238.

Lin, Y.P., Li, L., Zhang, F. & Linhardt, R.J. (2017) *Borrelia burgdorferi* glycosaminoglycan-binding proteins: A potential target for new therapeutics against Lyme disease. *Microbiology*, *163*, 1759–1766. Available from: https://doi.org/10.1099/mic.0.000571

Maghrabi, A.H.A. & McGuffin, L.J. (2017) ModFOLD6: An accurate web server for the global and local quality estimation of 3D protein models. *Nucleic Acids Research*, *45*, W416–W421.Available from: https://doi.org/10.1093/nar/gkx332

Morgan, A., Sepuru, K.M., Feng, W., Rajarathnam, K. & Wang, X. (2015) Flexible linker modulates glycosaminoglycan affinity of decorin binding protein A. *Biochemistry*, *54*, 5113–5119.Available from: https://doi.org/10.1021/acs.biochem.5b00253

Morgan, A.M. & Wang, X. (2015) Structural mechanisms underlying sequence-dependent variations in GAG affinities of decorin binding protein A, a *Borrelia burgdorferi* adhesin. *The Biochemical Journal*, *467*, 439–451.Available from: https://doi.org/10.1042/BJ20141201

Moriarty, T.J., Norman, M.U., Colarusso, P., Bankhead, T., Kubes, P. & Chaconas, G. (2008) Real-time high resolution 3D imaging of the lyme disease spirochete adhering to and escaping from the vasculature of a living host. *PLoS Pathogens*, *4*, e1000090. Available from: https://doi.org/10.1371/journal.ppat.1000090

Norman, M.U., Moriarty, T.J., Dresser, A.R., Millen, B., Kubes, P. & Chaconas, G. (2008) Molecular mechanisms involved in vascular interactions of the Lyme disease pathogen in a living host. *PLoS Pathogens*, *4*, e1000169. Available from: https://doi.org/10.1371/journal.ppat.1000169

Nyarko, E., Grab, D.J. & Dumler, J.S. (2006) Anaplasma phagocytophilum-infected neutrophils enhance transmigration of *Borrelia burgdorferi* across the human blood brain barrier in vitro. *International Journal for Parasitology*, *36*, 601–605.Available from: https://doi.org/10.1016/j.ijpara.2006.01.014

Pearson, W.R. (2013) An introduction to sequence similarity ("homology") searching. *Current Protocols in Bioinformatics*, *Chapter 3*(Unit3), 1. Available from: https://doi.org/10.1002/0471250953.bi0301s42

Pikas, D.S., Brown, E.L., Gurusiddappa, S., Lee, L.Y., Xu, Y. & Höök, M. (2003) Decorin-binding sites in the adhesin DbpA from *Borrelia burgdorferi*: A synthetic peptide approach. *Journal of Biological Chemistry*, *278*, 30920–30926.Available from: https://doi.org/10.1074/jbc.M303979200

Pulzova, L., Kovac, A., Mucha, R., Mlynarcik, P., Bencurova, E., Madar, M. et al. (2011) OspA-CD40 dyad: Ligand-receptor interaction in the translocation of neuroinvasive Borrelia across the blood-brain barrier. *Scientific Reports*, *1*, 86. Available from: https://doi.org/10.1038/srep00086

Robert, X. & Gouet, P. (2014) Deciphering key features in protein structures with the new ENDscript server. *Nucleic Acids Research*, *42*, W320–W324.Available from: https://doi.org/10.1093/nar/gku316

Roberts, W.C., Mullikin, B.A., Lathigra, R. & Hanson, M.S. (1998) Molecular analysis of sequence heterogeneity among genes encoding decorin binding proteins A and B of *Borrelia burgdorferi* sensu lato. *Infection and Immunity*, *66*, 5275–5285.Available from: https://doi.org/10.1128/IAI.66.11.5275-5285.1998

Sajanti, E., Virtanen, M., Helve, O., Kuusi, M., Lyytikäinen, O., Hytönen, J. et al. (2017) Lyme Borreliosis in Finland, 1995–2014. *Emerging Infectious Diseases*, *23*, 1282–1288.Available from: https://doi.org/10.3201/eid2308.161273

Sali, A. & Blundell, T.L. (1993) Comparative protein modelling by satisfaction of spatial restraints. *Journal of Molecular Biology*, *234*, 779–815. Available from: https://doi.org/10.1006/jmbi.1993.1626

Salo, J., Jaatinen, A., Söderström, M., Viljanen, M.K. & Hytönen, J. (2015) Decorin binding proteins of *Borrelia burgdorferi* promote arthritis development and joint specific post-treatment DNA persistence in mice. *PLoS One*, *10*, e0121512. Available from: https://doi.org/10.1371/journal.pone.0121512

Salo, J., Loimaranta, V., Lahdenne, P., Viljanen, M.K. & Hytönen, J. (2011) Decorin binding by DbpA and B of *Borrelia garinii*, *Borrelia afzelii*, and *Borrelia burgdorferi* sensu Stricto. *Journal of Infectious Diseases*, *204*, 65–73.Available from: https://doi.org/10.1093/infdis/jir207

Salo, J., Pietikäinen, A., Söderström, M., Auvinen, K., Salmi, M., Ebady, R. et al. (2016) Flow-tolerant adhesion of a bacterial pathogen to human endothelial cells through interaction with biglycan. *Journal of Infectious Diseases*, *213*, 1623–1631.Available from: https://doi.org/10.1093/infdis/jiw003

Stanek, G. & Strle, F. (2018) Lyme borreliosis-from tick bite to diagnosis and treatment. *FEMS Microbiology Reviews*, *42*, 233–258.Available from: https://doi.org/10.1093/femsre/fux047

Steere, A.C., Strle, F., Wormser, G.P., Hu, L.T., Branda, J.A., Hovius, J.W. et al. (2016) Lyme borreliosis. *Nature Reviews Disease Primers*, *2*, 16090. Available from: https://doi.org/10.1038/nrdp.2016.90

Tkáčová, Z., Pulzová, L.B., Mochnáčová, E., Jiménez-Munguía, I., Bhide, K., Mertinková, P. et al. (2020) Identification of the proteins of *Borrelia garinii* interacting with human brain microvascular endothelial cells. *Ticks and Tick-borne Diseases*, *11*, 101451. Available from: https://doi.org/10.1016/j.ttbdis.2020.101451

Tuominen-Gustafsson, H., Penttinen, M., Hytönen, J. & Viljanen, M.K. (2006) Use of CFSE staining of borreliae in studies on the interaction between borreliae and human neutrophils. *BMC Microbiology*, *6*, 92.

Wallner, B. & Elofsson, A. (2003) Can correct protein models be identified? *Protein Science*, *12*, 1073–1086.Available from: https://doi.org/10.1110/ps.0236803

Wang, X. (2012) Solution structure of decorin-binding protein A from *Borrelia burgdorferi*. *Biochemistry*, *51*, 8353–8362.

Weening, E.H., Parveen, N., Trzeciakowski, J.P., Leong, J.M., Höök, M. & Skare, J.T. (2008) *Borrelia burgdorferi* lacking DbpBA exhibits an early survival defect during experimental infection. *Infection and Immunity*, *76*, 5694–5705.Available from: https://doi.org/10.1128/IAI.00690-08

SUPPORTING INFORMATION

Additional supporting information may be found online in the Supporting Information section.

How to cite this article: Pietikäinen A, Åstrand M, Cuellar J, et al. Conserved lysine residues in decorin binding proteins of *Borrelia garinii* are critical in adhesion to human brain microvascular endothelial cells. *Mol Microbiol*. 2021;00:1–15. https://doi.org/10.1111/mmi.14687